Protoplasma (2003) 221: 153–161
DOI 10.1007/s00709-002-0058-z

PROTOPLASMA
Printed in Austria

Reduction of potassium tellurite to elemental tellurium and its effect on the plasma membrane redox components of the facultative phototroph *Rhodobacter capsulatus*

F. Borsetti, R. Borghese, F. Francia, M. R. Randi, S. Fedi, and **D. Zannoni** *

Department of Biology, University of Bologna, Bologna

Received May 2, 2002; accepted July 26, 2002; published online May 21, 2003

Summary. Anaerobically light-grown cells of *Rhodobacter capsulatus* B100 are highly resistant to the toxic oxyanion tellurite (TeO_3^{2-}; minimal inhibitory concentration, 250 μg/ml). This study examines, for the first time, some structural and biochemical features of cells and plasma membrane fragments of this facultative phototroph grown in the presence of 50 μg of K_2TeO_3 per ml. Through the use of transmission microscopy and X-ray microanalysis we show that several "needlelike" shaped granules of elemental tellurium are accumulated into the cytosol near the intracytoplasmic membrane system. Flash-spectroscopy, oxygen consumption measurements, and difference spectra analysis indicated that membrane vesicles (chromatophores) isolated from tellurite-grown cells are able to catalyze both photosynthetic and respiratory electron transport activities, although they are characterized by a low *c*-type cytochrome content (mostly soluble cytochrome c_2). This feature is paralleled by a low cytochrome *c* oxidase activity and with an NADH-dependent respiration which is catalyzed by a pathway leading to a quinol oxidase (Qox) inhibited by high (millimolar) concentrations of cyanide (CN^-). Conversely, membranes from *R. capsulatus* B100 cells grown in the absence of tellurite are characterized by a branched respiratory chain in which the cytochrome *c* oxidase pathway (blocked by CN^- in the micromolar range) accounts for 35–40% of the total NADH-dependent oxygen consumption, while the remaining activity is catalyzed by the quinol oxidase pathway. These data have been interpreted to show that tellurite resistance of *R. capsulatus* B100 is characterized by the presence of a modified plasma-membrane-associated electron transport system.

Keywords: Cytochrome; Flash spectroscopy; Respiration; *Rhodobacter capsulatus*; Tellurium inclusion; X-ray microanalysis.

Introduction

The oxyanion tellurite (TeO_3^{2-}) is highly toxic to prokaryotic and eukaryotic cells (Wagner et al. 1995, Turner 2001) at concentrations as low as 1 μg/ml (4 μM). Intrinsic low-level resistance to TeO_3^{2-} has been reported for a few Gram-positive bacteria such as *Corynebacterium diphtheriae* and *Streptococcus faecalis* (Summers and Silver 1978), while a constitutive high-level resistance at concentrations between 1 and 2.5 mg/ml (0.4–1 mM) has been found in several Gram-negative bacteria belonging to the class "Alphaproteobacteria" (Yurkov and Beatty 1998, Yurkov et al. 1996).

In Gram-negative bacteria, resistance to tellurite has been associated to at least five determinants, all apparently unrelated to one another at either DNA or protein level (Turner et al. 1995, Taylor 1999, Turner 2001). It has been largely documented that the majority of tellurite-resistant bacteria convert tellurite to elemental tellurium (reduction of Te^{IV} to Te^0) which is accumulated intracellularly as black inclusions (Taylor 1999). In this respect it was proposed that reduction of tellurite into less toxic elemental tellurium (Te^0) might represent a secondary pathway for detoxification; on the other hand, tellurite resistance without metal accumulation was observed in several species of phototrophic bacteria implying that tellurite resistance does not strictly depend on the formation of black inclusions of elemental tellurium (Yurkov et al. 1996).

The role assumed by respiratory and photosynthetic bacterial electron transport chains during tellurite reduction remains elusive, although several reports suggest that plasma membrane redox enzymes might be involved in at least one of the two enzymatic steps required to generate tellurium from tellurite (Moore

* Correspondence and reprints: Department of Biology, University of Bologna, Via Irnerio 42, 40126 Bologna, Italy.

and Kaplan 1992). The extent of tellurite reduction in *Rhodobacter sphaeroides* was inversely related to the oxidation state of the carbon source and it has also been shown to be dependent on reduced flavin adenine dinucleotide oxidation activity (Moore and Kaplan 1992, 1994). Chiong et al. (1988) have purified a protein fraction from *Thermus thermophilus* which contained an NADH/NADPH-dependent tellurite-reducing activity, while the membrane-bound nitrate reductases (NarG and NarZ) of *Escherichia coli* have been found to reduce tellurite and contribute to its basal level of resistance to the oxyanion (Avazeri et al. 1997). Additionally, the periplasmically located nitrate reductase (Nap) also exhibits tellurite reductase activity (R. J. Turner, pers. commun.). Recently, the electron transport flow catalyzed by the branched respiratory chain of *Pseudomonas aeruginosa* (Matsushita et al. 1980, Zannoni 1989, Cunningham and Williams 1995) has tentatively been correlated with reduction of potassium tellurite (Trutko et al. 2000). Further, strain KF707 of *Pseudomonas pseudoalcaligenes*, which is able to cometabolize polychlorinated biphenyls under aerobic conditions (Taira et al. 1992, Fedi et al. 2001), has recently been reported to be resistant to tellurite (MIC = 150 μg/ml, 0.4 mM) (Di Tomaso et al. 2002). Interestingly, membrane fragments isolated from *P. pseudoalcaligens* KF707 were shown to contain a branched respiratory chain which was functionally and structurally modified in cells grown in the presence of the oxyanion (Di Tomaso et al. 2002). This observation prompted us to test the effect of tellurite on the plasma membrane redox components of *Rhodobacter capsulatus*, a facultative phototroph which has been shown to grow anaerobically in the light in the presence of high amounts of tellurite (Yurkov and Beatty 1998). Here we report that the tellurite resistance of *R. capsulatus* is linked to an intracellular accumulation of granules of elemental tellurium; in addition, we show that membrane fragments (chromatophores) isolated from photosynthetically grown cells are endowed with photosynthetic and respiratory apparatuses which are modified by growth in the presence of tellurite. The results are discussed on the basis of our working hypothesis that tellurite might change the redox state of the respiratory chain at the quinone pool level.

Material and methods

Bacterial strain

Rhodobacter capsulatus B100 was grown anaerobically in the light at 30 °C in RCV-malate minimal salt medium as described previously (Zannoni et al. 1978). Anaerobic photosynthetic liquid cultures were made in completely filled screw-capped bottles with an incident light intensity of 200 W/cm^2. Growth in the presence of tellurite was obtained by addition of 50 μg of K_2TeO_3 per ml.

Preparation of membranes

Rhodobacter capsulatus B100 cells were harvested at the end of their exponential-growth phase (A_{660} = 0.9). Membrane fragments were prepared using a French pressure cell and ultracentrifugation as described previously (Zannoni et al. 1978) in 0.1 M N-tris[hydroxymethyl] methylglycine buffer (pH 7.5) containing 10 mM $MgCl_2$. Membranes were suspended at a known protein concentration in the same buffer and used immediately for both electron transport measurements and spectroscopic studies.

Protein and bacteriochlorophyll determinations

The protein content of the samples was determined by the method of Bradford (1976) with bovine serum albumin as a standard. The bacteriochlorophyll content was measured spectrophotometrically at 775 nm in acetone-methanol (7 : 2, v/v) extracts with an extinction coefficient of 75 mM^{-1} cm^{-1} (Clayton 1963).

Measurement of oxygen uptake and inhibitor titrations

Respiratory activities in membrane fragments were determined by monitoring oxygen consumption with a Clark-type oxygen electrode YSI 53 (Yellow Springs Instruments Inc., Yellow Springs, Ohio, U.S.A.) as detailed elsewhere (Daldal et al. 2001).

Spectral analysis of cytochrome content of membranes

The amounts of cytochromes in membrane fragments and soluble fractions were estimated by recording, at room temperature, reduced (with sodium dithionite) minus oxidized (with potassium ferricyanide) optical difference spectra. A Jasco 7800 spectrophotometer and the extinction coefficients $\varepsilon_{561-575}$ of 22 mM^{-1} cm^{-1} and $\varepsilon_{551-540}$ of 19 mM^{-1} cm^{-1} were used for *b*- and *c*-type cytochromes, respectively, except for flash spectroscopy (see legend of Fig. 4 and Discussion section).

Kinetic spectrophotometry

Absorbance changes induced by a xenon flash lamp (EG&G FX201, discharging a 3 μF capacitor charged to 1.5 kV, 4 μs pulse duration at half-maximal intensity) were measured by a single beam spectrophotometer equipped with a double grating monochromator (bandwidth, 1.5 nm). The photomultiplier was protected by a Corning glass 4/96 filter. A triggered shutter was used to gate the measuring beam. Data were acquired by a LeCroy 9410 digital oscilloscope interfaced to an Olivetti M240 computer. All the measurements were performed under controlled redox potentials with a calomel electrode for reference and a platinum electrode as the measuring one. The redox mediators were phenazine ethosulfate, phenazine methosulfate, 2,3,5,6-tetramethyl-*p*-phenylenediamine (DAD), *p*-benzoquinone, 1,2-naphthoquinone (1,2-NQ), and 1,4-

naphthoquinone (1,4-NQ) at the concentrations indicated in the legend of Fig. 4. To determine the stoichiometry of the photosynthetic redox components, trains of 14 flashes of light, 100 ms spaced, were used to photoactivate chromatophores in the presence of 3 μM valinomycin and 3 μM nigericin as uncouplers and 10 μM antimycin A to inhibit the cyclic electron flow.

Electron microphotographs of bacterial cells

To determine the presence of tellurium (Te^0) in bacterial cells, tellurite (50 μg/ml) was added to the liquid culture at the beginning of the exponential-growth phase. Ten hours later, when the bacterial cultures became black, they were harvested and processed for electron microscopy analysis as follows: cell pellets were fixed for 2 h in 0.05 M cacodylate, 1.5% (w/v) glutaraldehyde (pH 7.2); the same buffer was used for overnight washing of the samples followed by 2 h fixation with 2% (w/v) osmium tetroxide and dehydration with ethanol. Samples were finally embedded in Durcopan. Thin sections obtained by a LKB Ultratome Nova were double-stained with uranyl acetate and lead citrate (Reynolds 1963). Specimens were examined with a Philips CM-100 transmission electron microscope.

X-ray microanalysis

To obtain X-ray spectra, unstained specimen sections collected on a copper grid (200 mesh) and carbon coated were used. The specimen was analyzed with a Philips Tecnai F20 equipped with Edax Ultrathin Window energy dispersive spectrometer. The microscope was equipped with a field emission source and was operated at an accelerating voltage of 200 kV in the nanoprobe mode, thus minimizing both the beam broadening and the spurious X-ray signal coming from areas close to the one analyzed. All X-ray spectra were taken with the same count rate.

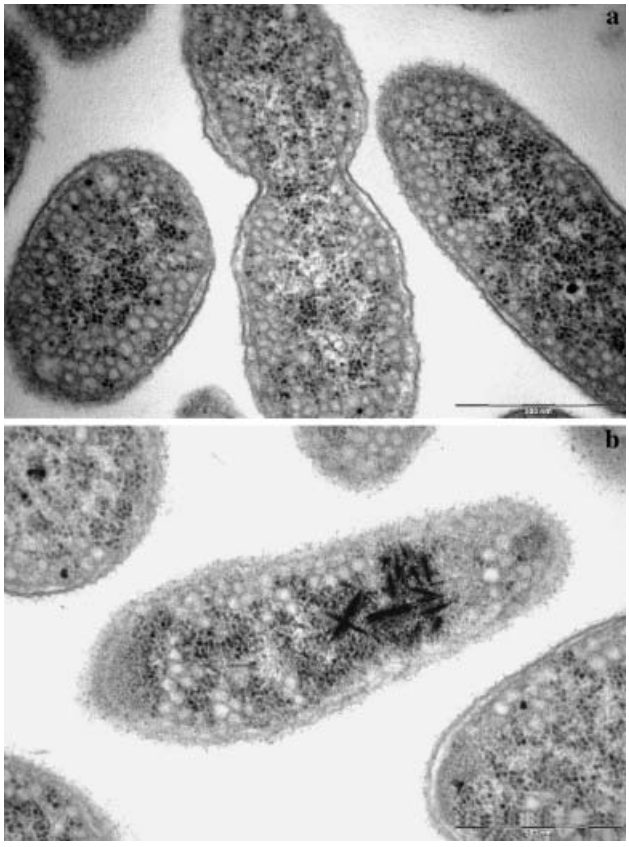

Fig. 1. Electron microphotographs of *R. capsulatus* B100 cells grown photosynthetically in RCV medium in the absence (**a**) or presence (**b**) of potassium tellurite. The tellurite-grown cells show electron-dense granules. Bars: 0.2 μm

Results

Electron microscopy

In Fig. 1 a and b, electron microphotographs of *R. capsulatus* cells grown photosynthetically in the absence or presence of potassium tellurite are shown. Apparently several electron-dense granules are present in the cytoplasm of cells which were harvested from liquid cultures supplemented with 50 μg of potassium tellurite per ml (Fig. 1 b), while control cells (Fig. 1 a) are clear of black inclusions. Notably, the "needlelike" shaped granules of tellurium in phototrophycally grown cells are located intracellularly close to the intracytoplasmic membrane system which is typical of cells grown anaerobically in the light (Drews and Golecki 1995).

X-ray microanalysis

The spectrum shown in Fig. 2 a was obtained by focusing the electron beam on the dark inclusions characterizing cells from tellurite-grown cultures (see Fig. 1 b). Apparently, L family lines of elemental tellurium are present between 3.6 and 4.5 keV; in addition, peaks corresponding to C, CuLα, and CuKα (Goldstein et al. 1981) can be seen at 0.285, 0.90, and 8.10 keV, respectively. In this regard, it should be noted that Cu lines were generated by the copper grid supporting the specimen, while the strong C line (at 0.285 keV) was due to both the thin carbon layer deposited on the sample and to the carbon contamination inside the microscope.

The control spectrum shown in Fig. 2 b was obtained by focusing the electron beam on a cytoplasmic region clear of dark inclusions. Clearly no tellurium peaks are present, while phosphorous and sulphur peaks (at 2.013 and 2.307 keV, respectively) typical of organic material are seen. As expected, carbon and copper peaks are also present; note that in Fig. 2 b the y-axis scale of the spectrum is approximately 1.5 times the one of the spectrum in Fig. 2 a.

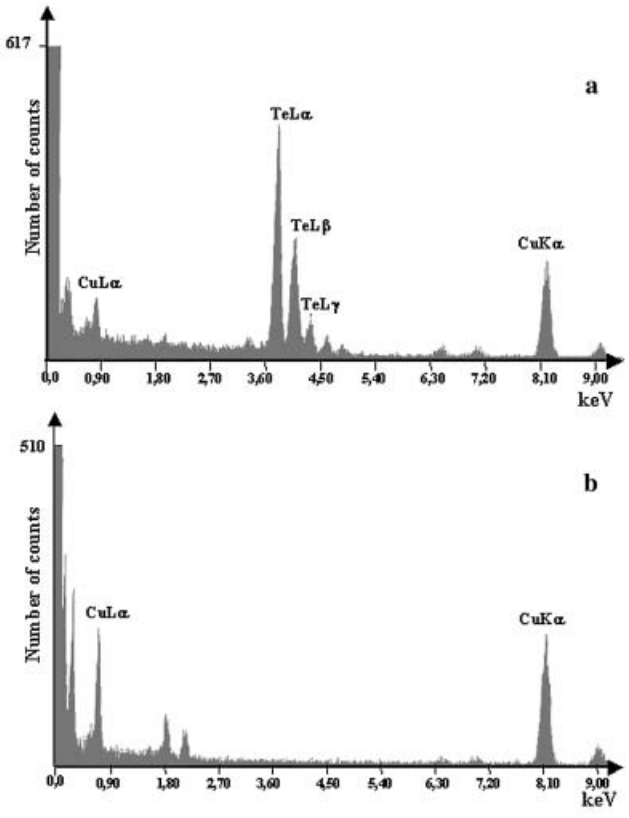

Fig. 2. X-ray microanalysis of the cytosolic content of *R. capsulatus* B100 cells grown photosynthetically in RCV medium in the presence (**A**) or absence (**B**) of potassium tellurite. For tellurite-grown cells the electron beam was focused on their characteristic dark inclusions. Note that in both panels the number of counts correspond to an acquisition time of 91 ms. Copper and carbon lines were due to specimen support and coat

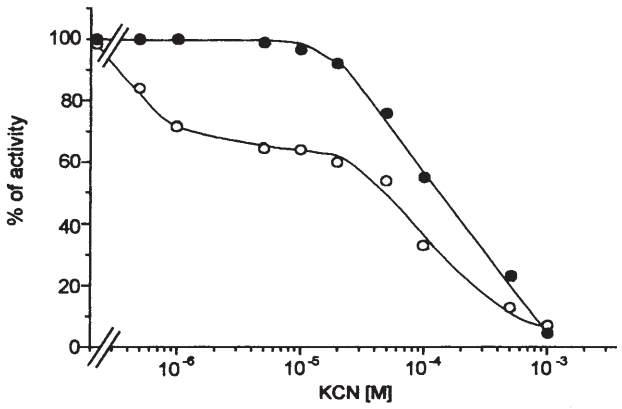

Fig. 3. Cyanide inhibition of the NADH-dependent oxidative activity in membranes from cells of *R. capsulatus* B100 grown photosynthetically in the presence (●) or absence (○) of potassium tellurite. See Table 1 for substrate concentrations

Respiratory activities in membrane fragments from R. capsulatus B100 cells grown in presence or absence of tellurite

Preliminary experiments were carried out to determine the respiratory activities of membrane fragments isolated from *R. capsulatus* B100 cells grown anaerobically in the light in the presence or absence of potassium tellurite (50 µg/ml) and harvested at their late-exponential-growth phase (optical density at 660 nm, 0.9). It has previously been shown that *R. capsulatus* strain St. Louis is endowed with a branched respiratory chain leading to two membrane-bound oxidases: one oxidase, which has either soluble cyt c_2 or membrane-attached cyt c_y as electron donors, is of cbb_3 type and is inhibited by low cyanide (CN^-) concentrations (micromolar range) (Zannoni et al. 1974, Gray et al. 1994); the other oxidase, which has quinol as electron donor, is inhibited by CO and by high CN^- concentrations (millimolar range) (Zannoni et al. 1976, Zannoni 1995) (see Fig. 6). To test for the presence of multiple membrane-bound oxidases in cells of strain B100, we have investigated the effect of cyanide on the NADH-dependent respiratory activity. The titers reported in Fig. 3 indicate that membranes from late-exponential-growth-phase cells grown in the absence of tellurite contain at least two terminal oxidases (byphasic curve) with different sensitivities to cyanide (50% inhibitory concentrations, 0.5 µM and 0.15 mM). Apparently, the cyanide-sensitive oxidase of strain B100 accounts for less than 35–40% of the total NADH-dependent respiration, while the cyanide-resistant oxidase (50% inhibitory concentration, 0.15 mM), the so-called alternative oxidase (Zannoni 1995), accounts for the rest of the respiratory activity. Figure 3 also shows that membranes isolated from cells grown in the presence of tellurite contain a cyanide-resistant oxidase contributing to almost the total NADH-dependent respiration; this result was also confirmed by the use of antimycin A, a specific inhibitor of the cyt bc_1 complex (Table 1). Table 1 also shows that the diversion of most of the electron transport flow through the cyanide-resistant oxidase did not affect at all the total NADH-dependent respiratory rate of membranes from tellurite-grown cells (6.6 µmoles of O_2 per h per mg of protein in both types of membranes), in spite of the fact that the cyt *c* oxidase (measured as ascorbate-horse heart cyt *c* oxidation) was 55% reduced in membranes from tellurite-grown cells (8.5 and 3.8 µmoles of O_2 per h per mg of protein, respectively).

Table 1. Oxidative activities of membranes from cells of *R. capsulatus* B100 photosynthetically grown in RCV medium in the presence or absence of 50 µg of potassium tellurite per ml

Electron donor	Inhibitor[a]	Oxidative activity[b] of membranes of cells grown in	
		RCV	RCV + K_2TeO_3
NADH (0.2 mM)	none	6.6	6.6
	antimycin A	3.3	6.4
	KCN	3.6	6.5
Succinate (2 mM)	none	5.3	5.4
	KCN	2.6	5.3
Asc (5 mM) + cyt *c* (60 µM)[c]	none	8.5	3.8
	KCN	0.5	0.1

[a] Concentrations: antimycin A, 5 µM; KCN (potassium cyanide), 10 µM
[b] Activities are expressed as µmoles of O_2 per h per mg of protein
[c] Na-ascorbate plus horse heart cytochrome *c*

Flash spectroscopy

The capacity of tellurite-grown cells of *R. capsulatus* B100 to generate through mechanical disruption (French pressure cell; see under Material and methods) orthodox sealed membrane vesicles (chromatophores) catalyzing a light-induced cyclic electron flow linked to the formation of an electrochemical membrane potential was investigated by flash spectroscopy.

Traces reported in Fig. 4 show the responses to a single actinic flash of light of the carotenoid band-shift (examined at 536 nm) (Fig. 4 a, a′), while the responses of cytochromes of *c*- (examined at 551–540 nm; Fig. 4 b, b′) and *b*-type (examined at 561–569 nm; Fig. 4 c, c′) and of the photosynthetic reaction center (RC) (spectroscopic signal at 605 nm; Fig. 4 d, d′) were induced by trains of fourteen actinic flashes separated by 100 ms. For the sake of clarity, the traces in Fig. 4 d and d′ were corrected taking into account the fraction of preoxidized RC at the potential indicated in the figure legend, assuming an $E_{m7.0}$ of +440 mV for the RC oxidized/reduced couple (Evans and Crofts 1974).

The carotenoid band-shift is a response to transmembrane electrochemical potential, and it can be used as an internal membrane probe to show the integrity of isolated membrane vesicles (chromatophores) in terms of proton-coupling. Indeed, in the presence of ionophores such as valinomycin and nigericin, the carotenoid band-shift is eliminated due to the collapse of the membrane potential.

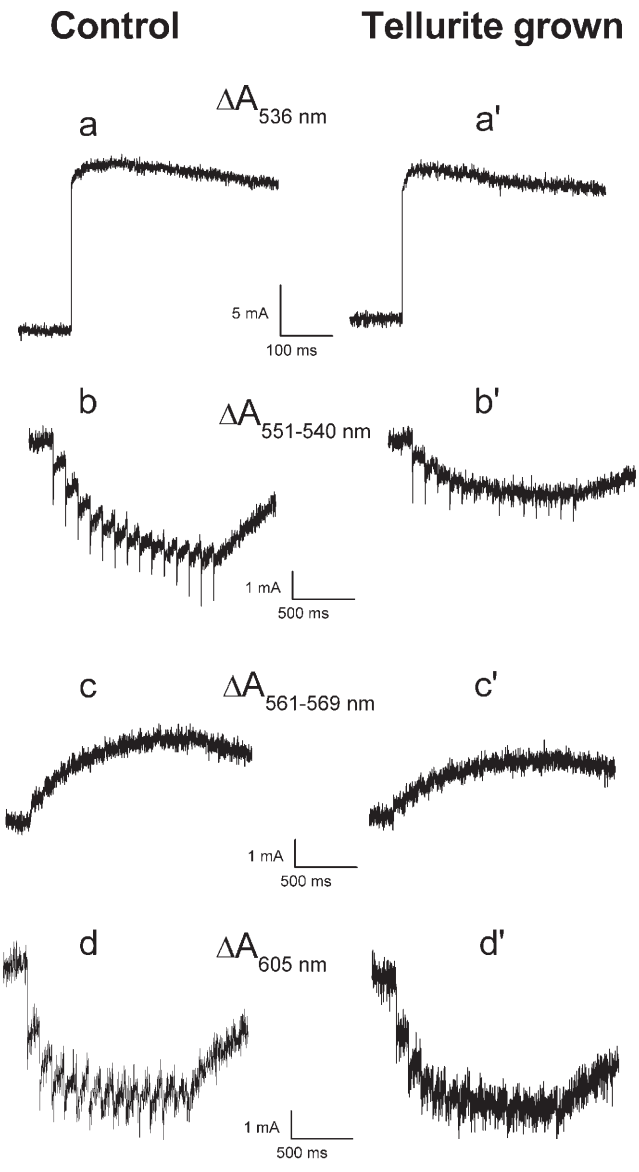

Fig. 4. Responses of the carotenoid band-shift (536 nm) (**a**), *c*-type cytochromes (551–540 nm) (**b**), *b*-type cytochromes (561–569 nm) (**c**), and photochemical RC (605 nm) (**d**), of membrane chromatophores from light-grown cells of *R. capsulatus* B100 to a single flash (**a**) or a train of fourteen actinic flashes of light (**b–d**). **a** and **a′** Measurements were performed on freshly prepared chromatophores suspended at a concentration of 80 µM bacteriochlorophyll in 50 mM morpholinepropanesulfonic acid, 100 mM KCl, pH 7.0 in the presence of 1 mM Na-ascorbate; 3 µM phenazine ethosulfate and 3 µM phenazine methosulfate, 10 µM DAD, 10 µM 1,2-NQ, and 10 µM 1,4-NQ were added as redox mediators. **b–d** and **b′–d′** Membranes were suspended in the same buffer at a concentration of 50 mM bacteriochlorophyll under redox controlled conditions in the presence of 3 µM valinomycin, 3 µM nigericin, 10 µM antimycin A; 2 µM DAD, 10 µM *p*-benzoquinone, 10 µM 1,2-NQ, and 10 µM 1,4-NQ were added as redox mediators. The E_h was +190 ± 10 mV (**b**, **b′** and **c**, **c′**), +428 mV (**d**), and +420 mV (**d′**). Kinetic traces were an average of 2 (**a** and **a′**) or 10 events (**b–d** and **b′–d′**)

Concerning the spectral signal of *c*-type hemes (cyt c_2 and c_y) (Zannoni 1995), it must be underlined that on the time scale used here, photooxidation of cytochromes *c* can be seen at a large extent only in the presence of the bc_1 inhibitor antimycin A (10 μM); in addition, under these experimental conditions, a consistent cyt *c* re-reduction should occur only after the first two turnovers, thus revealing the full extent of cyt *c* oxidation.

Figure 4 a and a′ shows that the carotenoid bandshift lasts for (at least) 500 ms after an actinic flash of light in both chromatophores from control and tellurite-grown cells demonstrating that both types of cells generate orthodox sealed membrane fragments through mechanical disruption (see under Material and methods). Figure 4 b and b′ shows that a consistent cyt *c* oxidation is produced after a series of actinic flashes of light in membranes from cells grown in the absence (control) or presence of tellurite; however, in the latter case, the extent of cyt *c* oxidation is approximately 50% of the control.

Antimycin A, which inhibits cyt *b* oxidation, is expected to reveal the maximal reduction of these cytochromes (signal at 561–569 nm). As shown in Fig. 4 c and c′, on a 500 ms time scale, the extent of cty *b* reduction in chromatophores from tellurite-grown cells is slightly less than that seen in the control trace. Notably, the RC photooxidation kinetics (seen at 605 nm) were similar in both membranes from control and tellurite-grown cells (Fig. 4 d, d′). This set of data has therefore been interpreted to show that *R. capsulatus* B100 cells grown in the presence of tellurite synthesize an orthodox intracytoplasmic membrane system. However, the amount of the *c*-type electron transport components (mainly soluble cyt c_2; see below) involved in photocyclic electron flow is far less than the one measured in membranes from control cells. During our studies we also noted that B100 chromatophore membranes showed a bacteriochlorophyll content (see under Material and methods) which was consistently 30% higher in tellurite-grown cells than in controls (on the basis of either RC or protein amounts).

Difference spectra

Reduced-minus-oxidized difference spectra (sodium dithionite as reducing agent) of membranes from B100 cells grown anaerobically in the light (optical density of 660 nm, 0.9) in the absence or presence of tellurite are shown in Fig. 5. The spectra were recorded from samples with identical protein concentrations (1 mg/ml) and are thus directly comparable. The presence of *c*- and *b*-type hemes with α-bands in their reduced form at 552 nm and 560 nm, respectively, is apparent. As expected from previous work (Zannoni 1995), in none of the spectra were signals observed which would have indicated the presence of aa_3-type hemes (α-band in their reduced form at 602–605 nm; not shown). As shown in Fig. 4, trace b the reduced-minus-oxidized difference spectrum of membranes isolated from cells anaerobically grown in the light in the presence of 50 μg of tellurite per ml is quantitatively different from control (Fig. 4, trace a). In particular, the α-band of *c*-type hemes at 552 nm is now considerably reduced compared to the one of *b*-type hemes (560 nm) with a cyt *c*/*b* ratio (on the basis of nmoles of heme per mg of protein) of 0.57, while the cyt *c*/*b* ratio in membranes from control cells is 0.95. These data, along with those obtained by flash-spectroscopic analysis, show clearly that the total *c*-type complement present in the plasma membranes isolated from tellurite-grown cells is considerably reduced by growth in the presence of tellurite. Further, comparing difference spectra of the crude cell extracts and soluble cell fractions (135000 **g**), it has been concluded that cells grown in the pres-

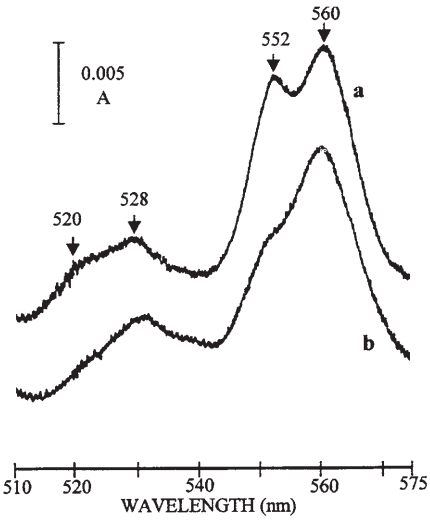

Fig. 5. Reduced-minus-oxidized difference spectra (recorded at 25 °C) of membrane fragments from cells of *R. capsulatus* B100 photosynthetically grown in RCV medium in the absence (trace *a*) or presence (trace *b*) of potassium tellurite. Samples were oxidized with a few crystals of K-ferricyanide and reduced with a few crystals of Na-dithionite. Protein concentration, 1 mg/ml

ence of tellurite contain less soluble cyt c_2 than control cells (decrease between 30% and 50% in 3 different membrane preparations; data not shown).

Discussion

In this study we have investigated some structural, spectroscopic and functional aspects of the plasma membrane system of *R. capsulatus* B100 cells grown photosynthetically in the presence of the toxic oxyanion tellurite.

The main results concerning the presence of dark inclusions in light-grown cells of *R. capsulatus* B100 can be summarized as follows: X-ray microanalysis demonstrated unequivocally that photosynthetic cells accumulate granules of elemental tellurium; tellurium inclusions (having a needlelike shape) are mainly located near the intracytoplasmic membrane system. This latter observation suggests a possible correlation between intracytoplasmic membrane and tellurite reduction (see also below). Indeed, the intracytoplasmic membrane system, which accommodates most of the photosynthetic and electron transport components, e.g., RC and Q/bc_1 complex (Drews and Golecki 1995), is likely to generate high amounts of reducing equivalents under anaerobic growth in the light. This might explain the presence of tellurium crystals clustered together inside the highly reducing cytosol region in contact with the intracytoplasmic membrane vesicles. In this respect, the present study also shows that the basic features characterizing the photosynthetic cyclic electron flow are not substantially altered by growth in the presence of tellurite. Indeed, membrane chromatophores generated by mechanical cell disruption (see under Material and methods) appeared to be sealed and the electron transfer kinetics are sensitive to inhibitors of the bc_1 complex. Since in the assay reported in Fig. 4 an equal amount of total RC has been evaluated in chromatophores from control and tellurite-grown cells (Fig. 4 d, d′), the latter contain far less (50%) photooxidizable cytochromes *c* (compare Fig. 4 b with b′). The *c*-type cytochromes interacting with the RC (cyt c_2 and c_y) can be estimated by subtracting from traces b and b′ the amount of cyt c_1 that corresponds to the total photoreducible cyt b_{561} of the bc_1 complex (Fig. 4 c, c′) taking into account the 1 : 1 stoichiometry between the c_1 and b_{561} prostetic groups. This can be done directly in Fig. 4, due to the equal values of the $\Delta\varepsilon_{551-540}$ and $\Delta\varepsilon_{561-569}$ (19.5 mM^{-1} cm^{-1}; Bowyer and Crofts 1981) putting in evidence how in tellurite-grown cells the *c*-type cytochromes interacting with the RC are dramatically reduced. Since photosynthesis and respiration share the same *c*-type complement (Zannoni 1995), the cyt *c* oxidase activity is also affected by the *c*-type heme decrease. In fact, in membranes from tellurite-grown cells, almost the entire NADH-dependent respiration is catalyzed by the cyanide-resistant respiration with a parallel reduction (55%) of the cyt *c* oxidase activity. A block scheme of the respiratory chain in membranes isolated from *R. capsulatus* B100 grown in the absence or presence of potassium tellurite is depicted in Fig. 6.

Although the mechanism of tellurite (TeO_3^{2-}) reduction by bacterial cells (a four-electron reaction) is as yet unknown (Turner 2001), a recent work on several tellurite-resistant aerobes (genera *Pseudomonas*, *Agrobacterium*, *Erwinia*, and *Escherichia*) proposed an active role of the respiratory chain in the accumulation of elemental tellurium; in addition, the periplasmic or cytoplasmic location of tellurium granules was correlated with the position of the catalytic centers of the terminal membrane-bound oxidases (Trutko et al. 2000). On the other hand, it was also shown that activation of the cyt *c* activity in cells of *Pseudomonas*

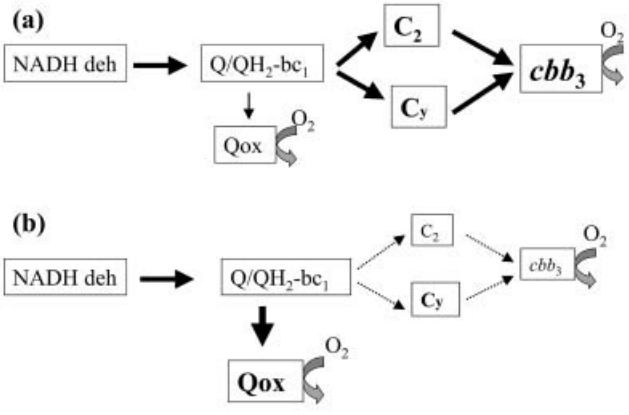

Fig. 6. Proposed block scheme of the respiratory electron transport system in cells of *R. capsulatus* B100 grown photosynthetically in RCV medium in the absence (**a**) or presence (**b**) of potassium tellurite. The thickness of solid arrows and letter size symbolize the relative rate of oxidative electron flow and cytochrome amount, respectively. Dotted arrows in **b** indicate the segment of the redox chain which is strongly repressed by tellurite addition. Notably, the Qox → O_2 branch (quinol oxidase pathway) is blocked by millimolar concentrations of cyanide, while the cbb_3 → O_2 (cyt *c* oxidase pathway) is blocked by micromolar concentrations of cyanide (see also Zannoni [1995] for further details). NADH deh, NADH dehydrogenase; Q, ubiquinone; QH_2, ubiquinol; bc_1, cyt bc_1 complex; c_2, soluble cyt *c*; c_y, membrane-attached cyt *c*; cbb_3, cbb_3 cyt *c* oxidase

aeruginosa lowers the cell Te content suggesting that reduction of tellurite and oxygen compete for the same pool of reducing equivalents at the Q/bc_1 level. Considering that potassium tellurite at pH 7.0 is mainly present in the form of $HTeO_3^-$ and TeO_3^{2-} (10^4/1 ratio, standard potentials of the redox couples estimated at –0.12 V at pH 7.0), the most likely thermodynamic interaction, if any, would be at the Q-pool level ($E_{m,7}$ of the redox couples $Q^{\bullet-}$/Q and Q/QH_2 of –200 and +90 mV, respectively). In this respect, it has previously been shown that the electron flow is modulated by changes in the Q-pool redox state only through the quinol oxidation site, Qo site, of the bc_1 complex (Venturoli et al. 1986). Further, under steady-state respiration, the bc_1 complex is reduced when the Q-pool reduction level reaches 4–5% of the total, whereas the quinol oxidase pathway (CN^--resistant oxidase) is operative only when the Q-pool is approximately 25% reduced (Zannoni and Moore 1990). Since we have shown (this work) that the cyt *c* oxidase activity in membranes from tellurite-grown cells of *R. capsulatus* B100 is significantly decreased as compared to control, it is likely to presume that this change would lead to an increase of the Q-pool reduction level and, as a consequence, to the quinol oxidase pathway (shown by the CN^- titers in Fig. 3). If our reasoning is correct, changes in the Q-pool redox state would also affect the photosynthetic apparatus since the Q-pool is intimately involved in the regulation of photosynthetic gene expression under both aerobic and anaerobic conditions. As previously shown by Gomelsky et al. (2000), in the presence of an external electron acceptor capable to directly oxidize the Q-pool, the increase of the Q oxidized state would decrease the expression of photopigment genes. In this respect our observation that tellurite-grown cells present a bacteriochlorophyll content higher (30%) than controls, suggests that under this growth condition the Q-pool is likely to be highly reduced, as expected by repression of the cyt *c* oxidase pathway, rather than oxidized (Zannoni and Moore 1990). Thus, although these data do not allow to establish whether or not the Q-pool redox level of *R. capsulatus* cells is modified by growth in the presence of tellurite, the increase of bacteriochlorophyll content in tellurite-grown cells might indirectly support this conclusion. On the other hand, the accumulation of black granules of tellurium inside the cells might interfere with the light intensity captured by phototrophic cultures and this shielding phenomenon could also affect the synthesis of antenna pigments (Drews and Golecki 1995). This aspect requires therefore further investigation.

The data presented raise the question whether the modifications observed are specifically required to survive in the presence of tellurite or simply reflect toxic effects of the oxyanion on metabolic pathways not directly related to the electron transport system. In other terms, the variations observed at the level of the plasma membrane redox components in cells grown in the presence of TeO_3^{2-} could be the result of a direct and/or indirect tellurite effect on genes coding for redox enzymes, a phenomenon not necessarily linked with the capacity of B100 to grow in the presence of tellurite. In this respect, it is difficult to explain why the strong decrease of the soluble *c*-type heme (cyt c_2) should better cope with cell survival in the presence of TeO_3^{2-}. On the other hand, the latter phenomenon has also been described in cells of *P. pseudoalcaligenes* KF707 grown aerobically in the presence of tellurite (Di Tomaso et al. 2002) and it appears therefore a typical adaptation of *Pseudomonas* and *Rhodobacter* species to growth in the presence of this oxyanion. Further studies are therefore necessary to establish whether modifications of the *c*-type heme complement are indicative of a functional response of the respiratory chain (possibly involved in tellurite reduction) by reduction of the electron flow through the cyt *c* oxidase pathway and enhancement of the quinol oxidative activity or they constitute a secondary effect of tellurite on metabolic functions such as for example *c*-type biosynthesis. Experiments aiming to define the response of the redox chain to tellurite in mutants with specific deletions at different levels of the respiratory system in *R. capsulatus* (Hochkoeppler et al. 1995) are in progress.

Acknowledgments

We thank MIUR for supporting this work (PRIN 2001). We also thank R. Balboni (CNR LAMEL Bologna I) and M. Manegatti for their skillful assistance with X-ray microanalysis.

References

Avazeri C, Turner RJ, Pommier J, Weiner JH, Giordano G, Vermeglio A (1997) Tellurite reductase activity of nitrate reductase is responsible for the basal resistance of *Escherichia coli* to tellurite. Microbiology 143: 1181–1189

Bowyer JR, Crofts AR (1981) On the mechanism of photosynthetic electron transfer in *Rhodopseudomonas capsulata* and *Rhodopseudomonas sphaeroides*. Biochim Biophys Acta 636: 218–233

Bradford MM (1976) A rapid and sensitive method for quantitation of microgram quantities of protein utilizing the principle of protein-dye binding. Anal Biochem 72: 248–254

Chiong M, Gonzales E, Barra R, Vasquez C (1988) Purification and biochemical characterization of tellurite-reducing activities from *Thermus thermophilus* HB8. J Bacteriol 170: 3269–3273

Clayton RK (1963) Toward the isolation of a photochemical reaction center in *Rhodopseudomonas sphaeroides*. Biochim Biophys Acta 75: 312–323

Cunningham L, Williams HD (1995) Isolation and characterization of mutants defective in the cyanide-insensitive respiratory pathway of *Pseudomonas aeruginosa*. J Bacteriol 177: 432–438

Daldal F, Mandaci S, Winterstein C, Myllykallio H, Duyck K, Zannoni D (2001) Mobile cytochrome c_2 and membrane-anchored c_y are both efficient electron donors to the cbb_3- and aa_3-type cytochrome *c* oxidases during respiratory growth of *Rhodobacter sphaeroides*. J Bacteriol 183: 2013–2024

Di Tomaso G, Fedi S, Carnevali M, Manegatti M, Taddei C, Zannoni D (2002) The membrane bound respiratory chain of *Pseudomonas pseudoalcaligenes* KF707 cells grown in the presence or absence of potassium tellurite. Microbiology 148: 1699–1708

Drews G, Golecki JR (1995) Structure, molecular organization, and biosynthesis of membranes of purple bacteria. In: Blankenship RE, Madigan MT, Bauer CE (eds) Anoxygenic photosynthetic bacteria. Kluwer, Dordrecht, pp 231–257

Evans H, Crofts AR (1974) In situ characterization of photosynthetic electron flow in *Rhodopseudomonas capsulata*. Biochim Biophys Acta 357: 89–102

Fedi S, Carnevali M, Fava F, Andracchio A, Zappoli S, Zannoni D (2001) Polychlorinated biphenyl degradation activities and hybridization analyses of fifteen aerobic strains isolated from a PCB-contaminated site. Res Microbiol 152: 583–592

Goldstein JI, Newbury DE, Echlin P, Joy DC, Fiori C, Lifshin E (1981) Scanning electron microscopy and X-ray microanalysis. Plenum, New York

Gomelsky M, Horne IM, Lee HJ, Pemberton JM, McEwan AG, Kaplan S (2000) Domain structure, oligomeric state, and mutational analysis of PpsR, the *Rhodobacter sphaeroides* repressor of photosystem gene expression. J Bacteriol 182: 2253–2261

Gray KA, Grooms M, Myllykallio H, Moomaw C, Slaughter C, Daldal F (1994) *Rhodobacter capsulatus* contains a novel *cb*-type cytochrome *c* oxidase without Cu_A center. Biochemistry 33: 3120–3127

Hochkoeppler A, Jenney FE, Daldal F, Zannoni D (1995) The membrane associated cytochrome c_y is essential for the respiratory chain of *Rhodobacter capsulatus*. J Bacteriol 177: 608–613

Matsushita K, Yamada M, Shinagawa F, Adachi O, Ameyama M (1980) Membrane-bound respiratory chain of *Pseudomonas aeruginosa* grown aerobically. J Biochem 88: 757–764

Moore MD, Kaplan S (1992) Identification of intrinsic high-level resistance to rare-earth oxides and oxyanions in members of the class *Proteobacteria*: characterization of tellurite, selenite, and rhodium sesquioxide reduction in *Rhodobacter sphaeroides*. J Bacteriol 174: 1505–1514

– – (1994) Members of the family *Rhodospirillaceae* reduce heavy-metal oxyanions to maintain redox poise during photosynthetic growth. ASM News 60: 17–24

Reynolds ES (1963) The use of lead citrate at high pH as an electron-opaque stain in electron microscopy. J Cell Biol 17: 208–212

Summers AO, Silver S (1978) Microbial transformation of metals. Annu Rev Microbiol 32: 637–672

Taira K, Hirose J, Hayashida S, Furukawa K (1992) Analysis of *bph* operon from the polychlorinated biphenyl-degrading strain of *Pseudomonas pseudoalcaligenes* KF707. J Biol Chem 267: 4844–4853

Taylor DE (1999) Bacterial tellurite resistance. Trends Microbiol 7: 111–115

Trutko SM, Akimenko VK, Suzina NE, Anisimova LA, Shlyapnikov MG, Baskunov BP, Duda VI, Boronin AM (2000) Involvement of the respiratory chain of gram-negative bacteria in the reduction of tellurite. Arch Microbiol 173: 178–186

Turner RJ (2001) Tellurite toxicity and resistance in Gram-negative bacteria. Rec Res Dev Microbiol 5: 69–77

– Weiner JH, Taylor DE (1995) The tellurite-resistance determinants *teh*A*teh*B and *kla*A*kla*B*tel*B have different biochemical requirements. Microbiology. 141: 3133–3140

Venturoli G, Fernandez-Velasco JG, Crofts AR, Melandri BA (1986) Demonstration of a collisional interaction of ubiquinol with the ubiquinol-cytochrome c_2 oxidoreductase complex in chromatophores from *Rhodobacter sphaeroides*. Biochim Biophys Acta 851: 340–352

Wagner M, Toews AD, Morell P (1995) Tellurite specifically affects squalene epoxidase: investigations examining the mechanism of tellurium-induced neuropathy. J Neurochem 64: 2169–2176

Yurkov V, Beatty JT (1998) Aerobic anoxygenic phototrophic bacteria. Microbiol Mol Biol Rev 62: 695–724

– Jappé J, Vermeglio A (1996) Tellurite resistance and reduction by obligately aerobic photosynthetic bacteria. Appl Environ Microbiol 62: 4195–4198

Zannoni D (1989) The respiratory chains of pathogenic pseudomonads. Biochim Biophys Acta 975: 299–316

– (1995) Aerobic and anaerobic electron transport chains in anoxygenic phototrophic bacteria. In: Blankenship RE, Madigan MT, Bauer CE (eds) Anoxygenic photosynthetic bacteria. Kluwer, Dordrecht, pp 949–971

– Moore AL (1990) Measurements of the redox state of the ubiquinone pool in *Rhodobacter capsulatus* membrane fragments. FEBS Lett 271: 123–127

– Baccarini-Melandri A, Melandri BA, Evans EH, Crofts AR (1974) The nature of the cytochrome *c* oxidase in the respiratory chain of *Rhodopseudomonas capsulata*. FEBS Lett 48: 152–155

– – – (1976) Further resolution of the cytochrome b type and the nature of the CO-sensitive oxidase present in the respiratory chain of *Rhodopseudomonas capsulata*. Biochim Biophys Acta 449: 386–400

– Jasper P, Marrs BL (1978) Light induced oxygen reduction as a probe of electron transport between respiratory and photosynthetic components in membranes of *Rps. capsulata*. Arch Biochem Biophys 191: 625–631

Verleger: Springer-Verlag KG, Sachsenplatz 4–6, A-1201 Wien. — Herausgeber: Dr. D. Menzel, Botanisches Institut und Botanischer Garten, Rheinische Friedrich-Wilhelms-Universität Bonn, Kirschallee 1, D-53115 Bonn, Bundesrepublik Deutschland. — Redaktion: Sachsenplatz 4–6, A-1201 Wien. — Satz und Umbruch: SNP Best-set Typesetter Ltd., Hong Kong. — Druck: Adolf Holzhausens Nachfolger, Holzhausenplatz 1, A-1140 Wien. — Verlagsort: Wien. — Herstellungsort: Wien. — Printed in Austria